AD-A108 504 MISSION RESEARCH CORP ALBUQUERQUE NM F/G 20/8
BEAM PROPAGATION EXPERIMENTAL STUDY.(U)
APR 81 C EKDAHL F49620-81-C-0016
UNCLASSIFIED AMRC-N-167 AFOSR-TR-81-0739 NL

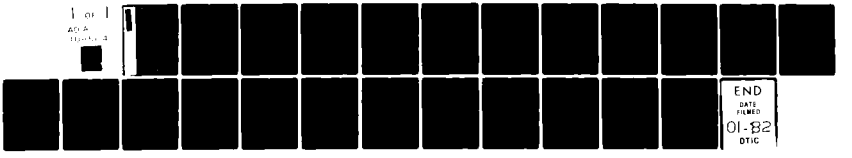

END
DATE FILMED
01-82
DTIC

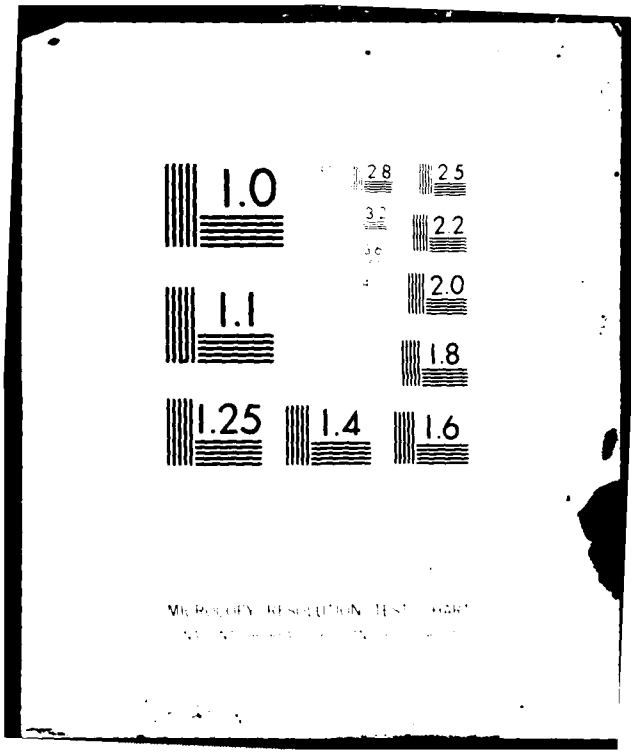
1.0
1.1
1.25
1.4
1.6
2.0
1.8
2.2
2.5

AFOSR-TR-81-0739

AMRC-N-167

INTERIM REPORT

BEAM PROPAGATION EXPERIMENTAL STUDY

Carl Ekdahl

08 April 1981

Prepared for: Air Force Office of Scientific Research
Physics Directorate
Bolling Air Force Base, D.C. 20332

Under Contract: F49620-81-C-0016

Prepared by: MISSION RESEARCH CORPORATION
1400 San Mateo Boulevard, S.E.
Suite A
Albuquerque, New Mexico 87108

UNCLASSIFIED

SECURITY CLASSIFICATION OF THIS PAGE (When Data Entered)

REPORT DOCUMENTATION PAGE		READ INSTRUCTIONS BEFORE COMPLETING FORM
1. REPORT NUMBER AFOSR-TR-81-0739	2. GOVT ACCESSION NO AD-A108504	3. RECIPIENT'S CATALOG NUMBER
4. TITLE (and Subtitle) BEAM PROPAGATION EXPERIMENTAL STUDY		5. TYPE OF REPORT & PERIOD COVERED Interim Report 6. PERFORMING ORG. REPORT NUMBER AMRC-N-167
7. AUTHOR(s) Carl Ekdahl		8. CONTRACT OR GRANT NUMBER(s) F49620-81-C-0016
9. PERFORMING ORGANIZATION NAME AND ADDRESS MISSION RESEARCH CORPORATION 1400 San Mateo Boulevard, S.E., Suite A Albuquerque, New Mexico 87108		10. PROGRAM ELEMENT, PROJECT, TASK AREA & WORK UNIT NUMBERS 61102F 2301/A7
11. CONTROLLING OFFICE NAME AND ADDRESS AIR FORCE OFFICE OF SCIENTIFIC RESEARCH Building 410 Bolling AFB, D.C. 20332		12. REPORT DATE 08 April 1981 13. NUMBER OF PAGES 25
14. MONITORING AGENCY NAME & ADDRESS(if different from Controlling Office)		15. SECURITY CLASS (of this report) Unclassified 15a. DECLASSIFICATION/DOWNGRADING SCHEDULE

16. DISTRIBUTION STATEMENT (of this Report)

APPROVED FOR PUBLIC RELEASE; DISTRIBUTION UNLIMITED

17. DISTRIBUTION STATEMENT (of the abstract entered in Block 20, if different from Report)

18. SUPPLEMENTARY NOTES

19. KEY WORDS (Continue on reverse side if necessary and identify by block number)

Relativistic electron beam propagation

Relativistic electron beam diagnostics

20. ABSTRACT (Continue on reverse side if necessary and identify by block number)

The pressure regime for stable propagation of an intense relativistic electron beam (I > 20 kA, W > 1.5 MeV, t > 20 ns) was determined and the beam-current density distribution was measured using an array of fast-response, subminiature Faraday cups. Experiments were performed on the stabilization of this pre-equilibrated beam when it was extracted into full-density air.

DD FORM 1 JAN 73 1473 EDITION OF 1 NOV 65 IS OBSOLETE

UNCLASSIFIED

SECURITY CLASSIFICATION OF THIS PAGE (When Data Entered)

INTRODUCTION

During February, 1981 the FX-25 accelerator was made available for development of diagnostics and exploratory propagation experiments. The diagnostic effort focused on the development of an array of subminiature Faraday cups for the determination of the beam spatial distribution. Experiments were also performed with a new technique for the measurement of the divergence of high energy density beams. In the propagation experiments the previously established range of pressures for stable propagation was confirmed for the particular geometry used; the beam spatial distribution was measured; and data was obtained on beam emittance. These measurements were made over a range of pressures that extended above and below the window for stable propagation. Finally, the beam was extracted into full density air after having propagated through the low pressure drift tube in order to investigate the effect on the hose instability of pulse sharpening, profile broadening, and phase mixing.

I. DIAGNOSTIC DEVELOPMENT

A. Subminiature Faraday-Cup Array

An array of fast-response Faraday-cup charge collecters was developed to measure the time-resolved current density spatial distribution. The use of this array allows the determination of the evolution of the radial beam profile on a single shot. The array used for the measurements reported here consisted of several coaxial Faraday collectors embedded in a carbon beam stop and shielded from the plasma electrons with a thin carbon sheet. The use of subminiature charge collectors eliminates the noise and response time problems associated with the detection of high currents. Furthermore, using a coaxial collector driving a matched and terminated signal cable provides the fastest possible response time. The response time of the signals observed in this experiment was limited by the bandwidth of the oscilloscopes to ~1 ns. The high signal level and unbroken coaxially-shielded construction gave essentially noise-free oscillograms.

Graphite was used throughout the design because of its superior resistance to damage by the high energy density beam. In a further development of this design, which had equivalent performance, the insulating gap, t_g, was replaced with a thin sheet (25 μm) of Kapton, which also had a high resistance to damage in this intense beam. A large version of this array has been constructed for use in the FX-100 experiments.

Electron scattering in the probe materials make it difficult to accurately predict the effective area of the coaxial charge collecter. Existing Monte Carlo electron-transport codes are being investigated as a means for establishing the sensitivity of the probes. This calibration was established experimentally for the FX-25 array by normalizing current density distributions measured close to the diode (Fig. 2) to the total diode current (measured with a resistive shunt). The same procedure will be used to experimentally calibrate the FX-100 array.

B. Faraday Cup Beam-Emittance Measurements

A new technique for making a time resolved measurement of the beam emittance was experimented with on the FX-25. Consider the geometry of Figure 1 with the thin carbon sheet (t_c) removed and the UT-47 solid coax retracted into the hole in the carbon block to a depth, δ, from the front surface. If the carbon were a perfect absorber then the only electrons that would be collected would be those with angles of incidence less than $\tan^{-1} D/2\delta$. A set of such probes retracted to different depths would thus provide a quantitative time-resolved measurement of the angular distribution of the incident beam. In fact, scattering in the carbon complicates the interpretation of the data obtained with this geometry and without elaborate Monte Carlo calculations, the results of the measurements made on the FX-25 can be only considered crude estimates, at best. Even using the scattering by known foil thicknesses as a means of establishing an empirical calibration does little to reduce the difficulty in interpreting data collected with this geometry. These preliminary experiments did, however, result in an improved design that should give easily interpreted data, and has been constructed for the FX-100

experiments. In this apparatus the coax charge collectors are set at the bottom of conical (rather than cylindrical) holes with varying cone angles. The depth of each hole is the same and is greater than one practical range in carbon for the FX-100 electron energy. This should sharpen the angular discrimination lacking in the previous design. Multiply-scattered electrons, secondaries, and plasma electrons will be discriminated against by use of a Kapton insulated tantalum sheet over the end of the coax detecter. An experimental calibration will be effected by exposing the array to the FX-100 beam scattered in anode foils of known thickness. This will be backed up with Monte Carlo scattering calculations.

II. PROPAGATION EXPERIMENTS

The propagation experiments reported here were performed in reduced pressure air in a 5-cm inner diameter, 307-cm long conducting drift tube. A graphite Rogowski surface cathode was used with a 25-μm Ti foil anode to produce a ~20 μs, 20 - 25 kA, 1.5 - 2.0 MeV beam from the FX-25 accelerator (Fig. 2). It has been previously established that the pressure window for stable propagation for this accelerator is 1 - 2 Torr. This was confirmed for this particular geometry by measurements of the beam energy deposited in a graphite calorimeter especially constructed for these experiments. The maximum energy was deposited in the calorimeter when the drift tube pressure was 1.6 Torr. This was only about 15 - 20% of the initial beam energy. The reason for this inefficient transport became clear when time-resolved measurements of the current density at 3 m were made. As seen in the data for the on-axis probe (Fig. 2) there was no pressure for which the full ~20 ns diode-current pulse width was propagated to the end of this drift tube. At the lower pressures, erosion of the beam head shortened the pulse from the maximum width of ~12 - 15 ns observed at ~1.6 Torr, while at higher pressure the hose instability eroded the tail of the beam as well. This overlap of the pressure regimes for severe nose erosion and hose instability was not observed on earlier FX-25 experiments with larger-diameter drift tubes, and is probably a result of the small-diameter tube used for these experiments.

The beam distribution at peak current evolved into a Bennett-like profile at the end of the drift tube as shown in Figure 4. The Bennett radius for the beam propagated in 1.6 Torr air inferred from these data is ~0.5 cm, and corresponds closely to the radius inferred from damage to dielectric foils (Fig. 4). However, the radius inferred from open shutter photographs of N_2^+ fluorescence at 3914 Å is about a factor of two greater, probably as a result of excitation by lower energy secondaries and plasma electrons.

As the pressure was reduced below 1.6 Torr into the regime of severe erosion of the beam, the profile broadened (Fig. 5), and an increase of current transported in the wings was observed. The inferred Bennett radius increased with reduced pressure until it was approximately equal to the tube radius at a pressure of ~0.8 Torr.

The total beam current inferred from the distribution profiles and maximum current rate of change are shown in Figure 6. It is seen here that although the current may be sharpened by erosion at lower pressures, the reduction in current results in an overall reduction in the rate of change.

III. BEAM EXTRACTION EXPERIMENTS

To date, all high intensity beams extracted directly from the diode into full density air have been observed to become hose unstable within a few (1 - 4) betatron wavelengths. The betatron wavelength is $\lambda_\beta \sim 2\pi a (I_A/I_{net})^{\frac{1}{2}}$, where I_{net} is the net (beam plus plasma) current, "a" is the Bennett equilibrium radius, and $I_A = \gamma\beta mc^3/e$ is the Alfven current. Therefore, effects that increase the equilibrium radius (such as increased beam emittance from foil scattering) have been observed to increase the hose-free propagation distance in previous experiments. Thick foil scattering also appears to have increased the number of betatron wavelengths before hose disruption, perhaps because of a reduction in growth rate resulting from more rapid phase mixing of the betatron motions. Finally, it is noted that a reduction of I_{net} will also increase λ_β and thus the hose-free propagation distance.

Extraction of the FX-25 beam into full-density air after it propagates through the 3-m low-pressure drift cell could be expected to produce a more stable beam by some combination of the aforementioned effects. The beam was observed to have a higher emittance at the end of the drift tube than at the diode. Furthermore, at the lower pressures the observed larger Bennett equilibrium radius would favor a larger hose-free propagation path. Finally, erosion-sharpened beam fronts could produce higher conductivity (as a result of avalanching in the high induction field) that in turn would result in reduced net currents and the associated increased λ_β.

To test the possibility of stabilizing the hose by pre-equilibration in a low-pressure propagation cell, the FX-25 beam was extracted through a 25-μm Kapton foil at the end of the 3-m drift tube. As the propagation-cell air pressure was reduced from slightly above the propagation window to slightly below, a marked stabilization of the hose was observed (Fig. 7 - 10) at pressures $\lesssim$1 Torr. Hose-free propagation was observed below this threshold until the beam struck the shield-block wall ~1 m from the exit point. (Presumably, if the available space for propagation were greater, then the extracted beam would eventually destabilize.) Hose stabilization in these experiments apparently resulted from increased emittance and Bennett-equilibrium radius at the reduced pressures. Enhanced conductivity was probably not contributory, because, as shown in Figure 6, the rate-of-change of beam current did not increase significantly as the cell pressure was dropped.

In conclusion, the availability of time on the FX-25 made it possible to develop two of the more important diagnostics required for the forthcoming FX-100 propagation experiments. A limited set of propagation experiments in a 3-m drift tube was performed that indicated an increased Bennett equilibrium radius at pressures below the pressure for maximum beam energy transport. This effect was used to stabilize the beam extracted into full-density air.

The author wishes to acknowledge the assistance of Winston Bostick in performing these experiments, especially in the development stages of the subminiature Faraday collectors.

This research was sponsored by the Air Force Office of Scientific Research (AFSC) under contract F49620-81-C-0016. Professor Bostick is a senior research physicist in the University Residency Research Program sponsored by the Air Force Office of Scientific Research under IPA-905-79-01016C.

Figure 1. Subminiature Faraday collector for beam current density measurements. The graphite shield thickness (t_c = 1.8 mm) is sufficient to stop electrons with energies less than 700 keV. An insulating gap (t_g = 1.7 mm) is provided between the shield and the graphite beam stop, which houses the array of rigid coaxial cable (UT-47) detectors. These have solid copper outer (D = 1.2 mm) and inner (d = 0.29 mm) conductors, and Teflon insulation.

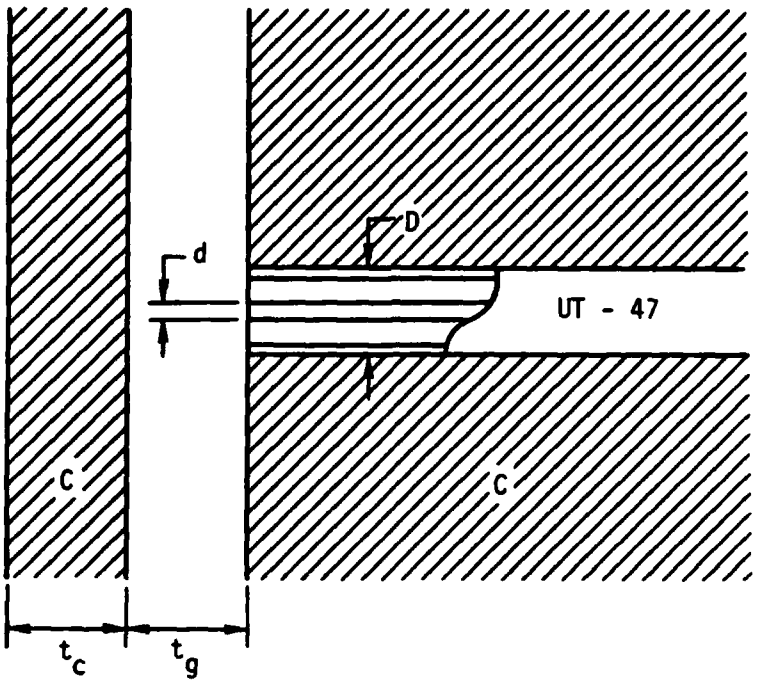
d
D
UT - 47
C
C
t_c
t_g

Figure 2. FX-25 diode geometry and beam current density profile measured in vacuum 0.5 cm from the titanium anode foil. The 51-μm anode foil induces a mean scattering angle of 16-20°. The current density profile shown was obtained at the time of peak current (I_{max} = 22 kA). The FX-25 produced beams having nominal values for parameters shown.

MRC

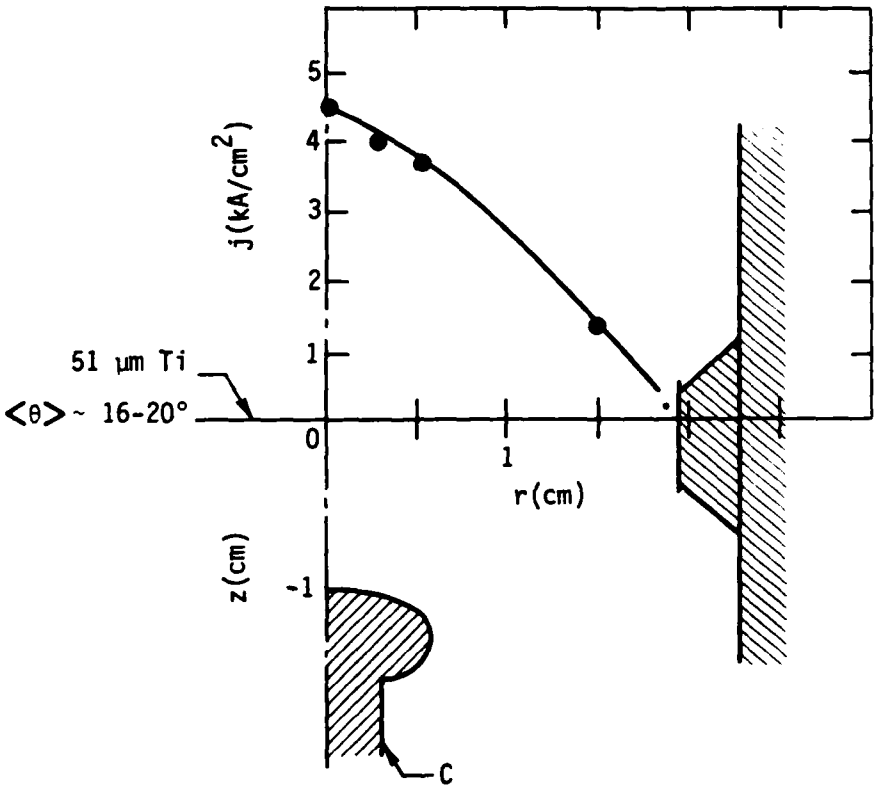

FX-25

1.5-2.0 MeV

20-25 kA

Δt ~ 20 ns

t_r ~ 5 ns

Figure 3. Beam current density on axis for different pressures near the propagation window. The current density near the diode had a waveform that approximated the envelope of these signals. The erosion of the beam nose is clearly evident at pressures below 1.6 Torr (upper). At higher pressures both nose erosion and tail loss resulting from hosing are evident (lower). (lower).

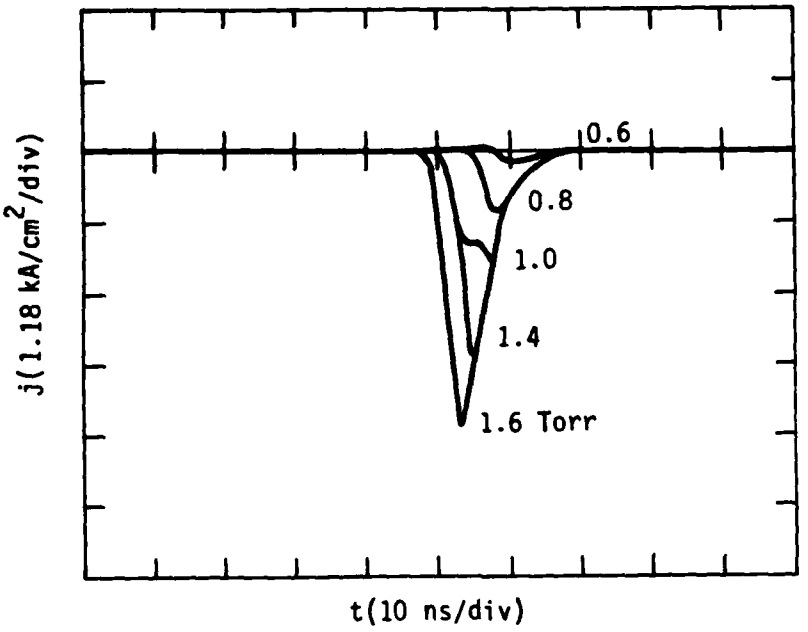
0.6
0.8
1.0
1.4
1.6 Torr
j(1.18 kA/cm^2/div)
t(10 ns/div)

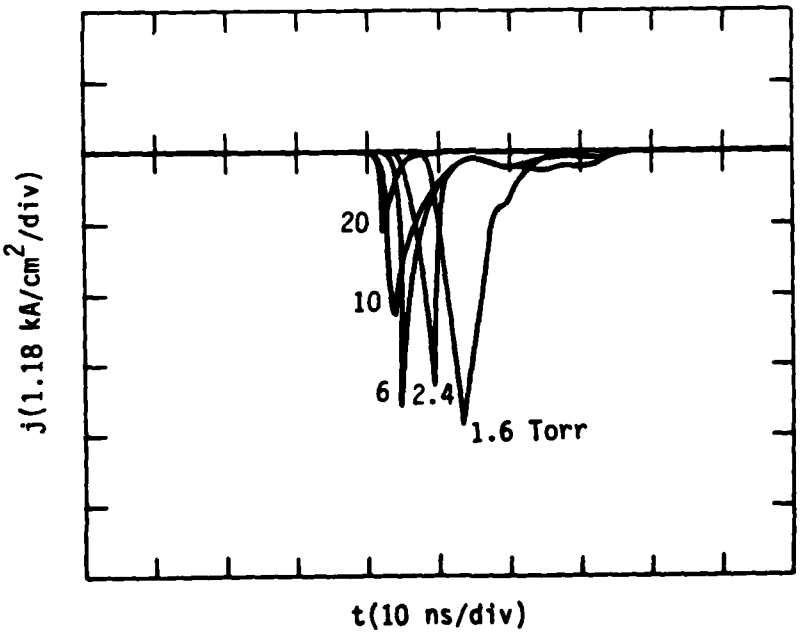
20
10
6
2.4
1.6 Torr
j(1.18 kA/cm^2/div)
t(10 ns/div)

Figure 4. Evolution of the beam current distribution near the diode (upper figure) into a Bennett-like profile (lower figure) after propagating 3-m in 1.6-Torr air (the pressure for maximum energy transport). Also shown are the range of radii determined from damage to dielectric foils (centered at r ~ 0.5 cm), and determined from extent of 3914 Å (N_2^+) emission (centered at r ~ 1 cm).

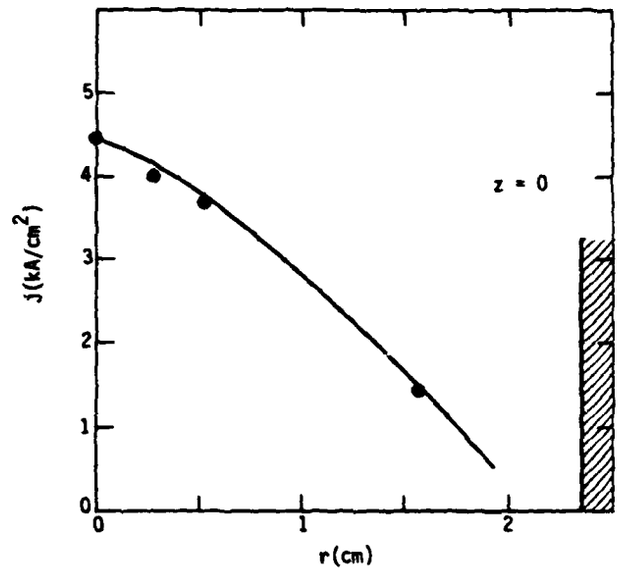
z = 0
J(kA/cm²)
r(cm)
0
1
2
3
4
5

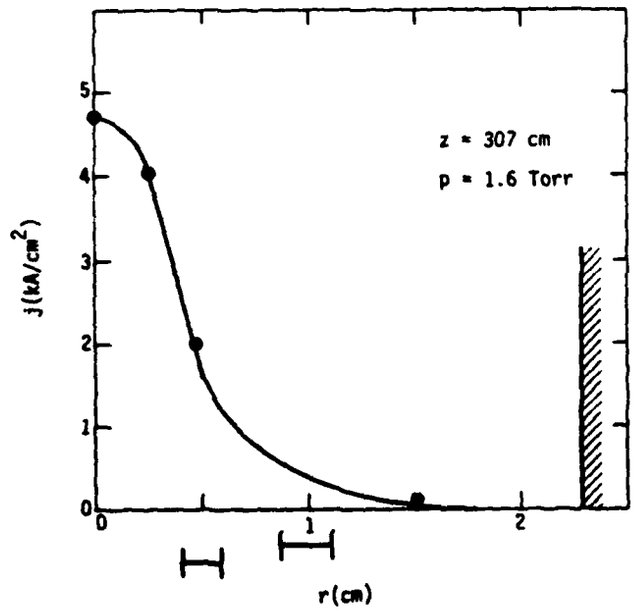
z = 307 cm
p = 1.6 Torr
J(kA/cm²)
r(cm)
0
1
2
3
4
5

Figure 5. Beam current distributions at 3 m for several air pressures. Maximum energy transport was observed at 1.6 Torr. The increased current density in the wings of the profiles at lower pressures was an effect noted on all of the shots at these pressures.

MRC

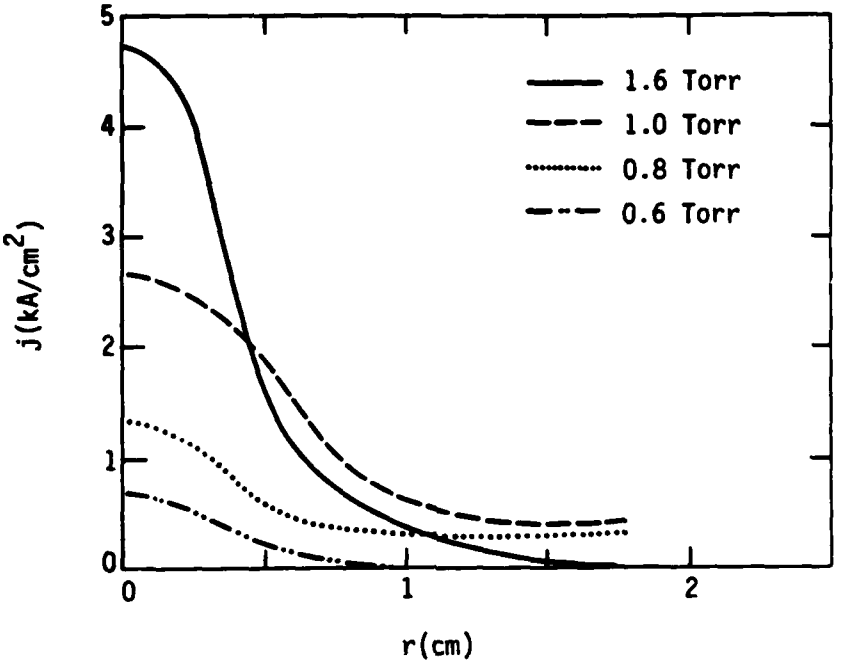

Figure 6. (Upper figure) Total beam current at the end of 3 m. These data were obtained by integrating the current distributions measured with the array of miniature Faraday cups. (Lower figure) Maximum time rate-of-change of the beam current at the end of the three meter drift tube.

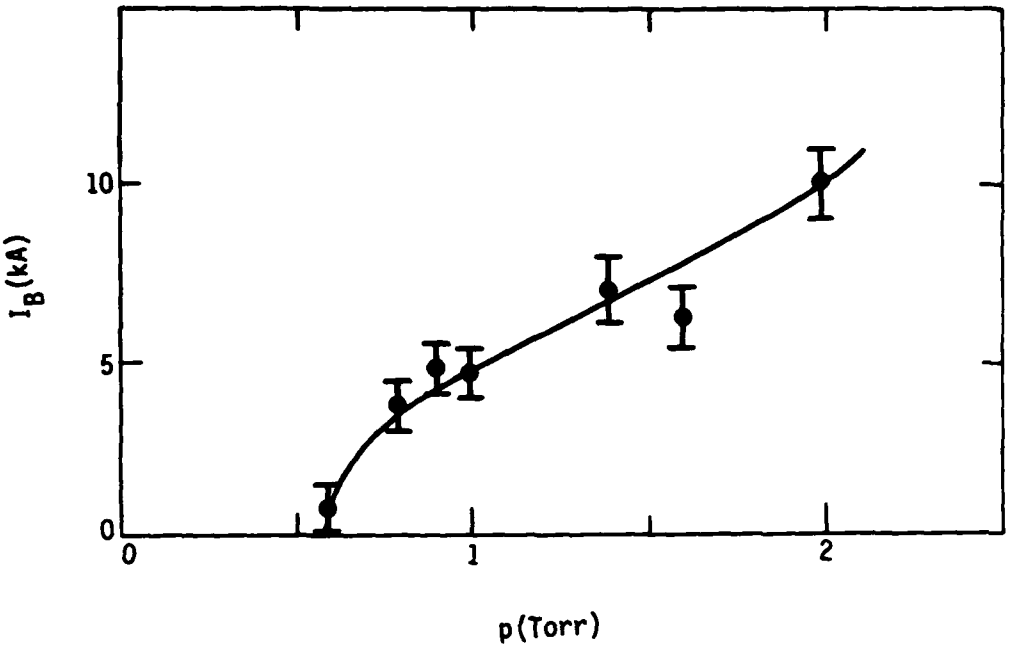
I_B(kA)
10
5
0
0
1
2
p(Torr)

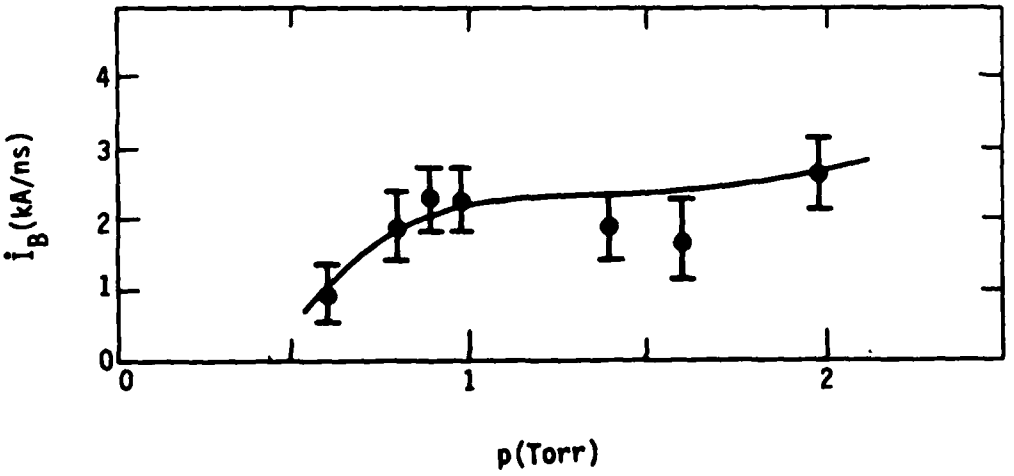
$\dot{I}_B$(kA/ns)
4
3
2
1
0
0
1
2
p(Torr)

Figure 7. Open shutter (time integrated) photograph of FX-25 beam extracted into full-density air (630 Torr) through a 25-μm Kapton foil after propagating 3-m in a 5-cm diameter conducting drift tube. The air pressure in the drift tube was 1.6 Torr, the pressure for maximum beam energy transport. The beam in the drift tube is visible through the round port on the drift tube.

Figure 8. Open shutter photograph of the FX-25 beam extracted into full-density air after drifting through 3-m of 0.8 Torr air.

Figure 9. Open shutter photograph of the FX-25 beam extracted into full-density air after drifting thorough 3-m of 3-Torr air.

Figure 10. Open shutter photograph of the FX-25 beam extracted into full density air after drifting through 3-m of 0.6-Torr air.


DATE
ILME